Three-dimensional vision using structured light applied to quality control in production line

L.-S. Bieri and J. Jacot

Ecole Polytechnique Federale de Lausanne, STI-IPR-LPM, Lausanne, Switzerland

ABSTRACT

Traditional backlighting vision systems are unable to measure the height dimensions of an object. It can then be more convenient to use a 3D scanner, based for example on the projection of structured light. Despite the high potential of this technique and the growing demand of the industry for performing quality vision control, 3D measurement systems are still often considered as unusual solutions.

This proceeding presents our 3D measurement laboratory setup based on the projection of structured light by means of a LCD beamer. This system is intended to be used in automated assembly line. The height information comes from a phase map obtained through temporal phase unwrapping. This phase always contain noise. Part of this noise brings a random phase error. A simple estimator of the random phase error is presented. It gives two parameters to which it is necessary to pay attention in order to predict measurement repeatability and thus to improve it. The estimator is experimentally validated on our setup.

Keywords: shape measurement, dimensional measurement, structured light, 3D scanner, quality control, temporal phase unwrapping

1. INTRODUCTION

The quality control of a product at any stage of the fabrication process consists of verifying its conformity regarding preset and quantified functional requirements. Depending on the results of this control, the sample can be rejected. In an automated production line, these controls must be automatic (no human intervention), flexible (easy adaptation of parameters when a change of batch occurs) and rapid.

Backlighting is mostly encountered for contactless dimensional measurements. It is based on the detection and analysis of the object outlines. This technique is easy to use but cannot measure height dimensions like the depth of a hole. In this case, 3D vision techniques are employed. The most often encountered are the laser line scanning and the projection of structured light in form of grids. As production line needs rapid measurement, the structured light technique is more convenient than the laser line which needs a number of images directly proportional with the required precision. Most existing systems based on structured light do not offer easy adaptation of paramters. They can only be used as black boxes whose functioning is generally bad understood by the user. However, the demand of performing quality control is growing in industry. It is thus important to make this kind of 3D acquisition techniques easier to use and to facilitate their implementation as complement to common 2D backlighting technique.

The Laboratoire de Production Microtechnique (LPM) of the Swiss Federal Institute of Technology (EPFL) is active in the domain of vision control techniques and mathematical tools used in decision stage (modelling). A 3D measurement setup has been developed. It is dedicated to dimensional control of little objects ($1cm$ side) of any color but not transparent. The goal is to obtain a precision of approximately $\pm 10\mu m$. The setup uses projection of structured light and height information is obtained from phase maps using temporal phase unwrapping. To ensure the measurement precision, we will address key question like "what confidence can we have in this height information ?" It is important for any measurement system to determine the error sources and their influence.

Further author information: (Send correspondence to L.S. Bieri)
L.S. Bieri: E-mail: louis-severin.bieri@a3.epfl.ch, Telephone: +41 21 693 59 46
Address: EPFL - Ecublens, STI-IPR-LPM, CH-1015 Lausanne, Switzerland

This proceeding summarizes the technics of phase acquisition and phase unwrapping used in our setup, presents an adaptation of the projection to improve the phase quality, and proposes a simple estimator of the random phase error. This estimator gives two parameters to which it is necessary to pay attention in order to minimize the random phase error and improve measurement repeatability. This estimator is experimentally validated on our setup.

2. HEIGHT MEASUREMENT BY PROJECTION OF STRUCTURED LIGHT

2.1. Generalities

Some light is said to be structured if it is spatially modulated in intensity (ex: the sunlight passing through a blind). The geometry of an object's visible part is determined with such structured light projected along a distinct axis than which of the measuring camera. This method consists in identifying, for each pixel on the camera, a virtual inclined plane which intersects the locally observed surface (fig.1 a). Representing each inclined

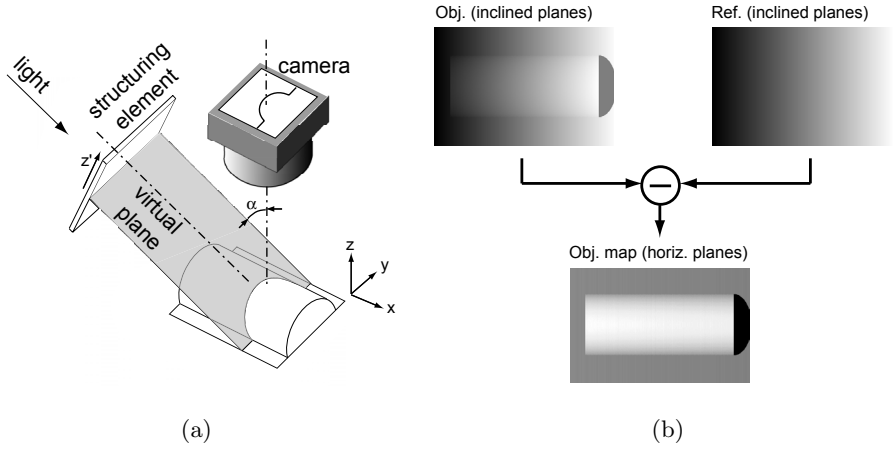

Figure 1. a) Representation of an inclined plane and its intersection with the surface object perceived by the camera. b) The difference between an image identifying the inclined plane which intersect the object and an image identifying the inclined plane which intersect the reference surface gives an image containing horizontal height levels of the object.

plane with a logical value (grayscale) we obtain the result shown in the top left side of the figure 1 b). A reference image (without object) is then subtracted to obtain an image in which each logical value identifies an horizontal height level as in a geographical map (fig.1 b). The height information being contained in the light, shadow areas are not informative.

2.2. Phase stepping

A robust identification of the inclined planes is obtained by computing the phase of sinusodal projected grids. If we successively project 3 shifted grids with sinusodal profile, of same frequency, the 3 images I_1, I_2 and I_3 taken by the camera allow the calculation of the phase by the phase stepping formula :

$$\varphi = \arctan\left(\sqrt{3} \cdot \frac{I_2 - I_3}{2I_1 - I_2 - I_3}\right) \tag{1}$$

as shown in figure 2 a). I_1, I_2 and I_3 are chosen so that the corresponding phase goes from $-\pi$ and π. This phase identifies each inclined plane without ambiguity. An error $\Delta\varphi$ produces an error Δz given by

$$\Delta z = \Delta\varphi \cdot dz/d\varphi. \tag{2}$$

Its effect can be reduced by increasing the sensibility $\frac{dz}{d\varphi}$, that means increasing the frequency of the projected grids. We can see on the figure 2 b) with $z' = z \cdot sin(\alpha)$ that this phase, limited by the equation 1 between $-\pi$ and π, presents some jumps and must be unwrapped by adding the correct multiple of 2π.

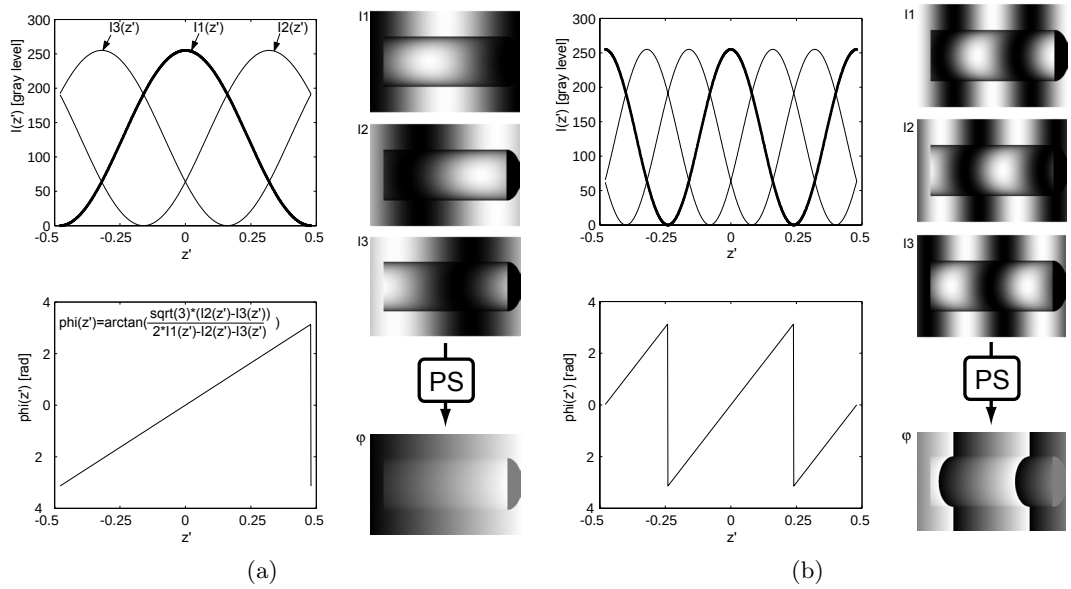

Figure 2. a) 3 sinusodal signals I_1, I_2 and I_3 of one period but shifted between each of them of $2\pi/3$ allow to compute a phase φ by the equation of phase stepping. The z' coordinates is this represented on the figure 1 b), z'=-0,5 and z'=0,5 identifying the limits of the structuring element. The signals are chosen so that the phase is included between $-\pi$ to π. b) If the sinusodal signals have more than one period, the phase present some jumps.

2.3. Temporal phase unwrapping

A wrapped phase image can be unwrapped spatially (2D unwrapping) but this approach is not very reliable in practice and produces often unwrapping errors which are detectable only by human control. This unwrapping technique is not compatible with our objective of automation. From this point, the temporal phase unwrapping (TPU), presented in detail by Saldner and Huntley,[1, 2] is more convenient. It consists of unwrapping a phase with high sensitivity by means of other phasees with lower sensitivity. The unwrapping, independently realized on each pixel, is robust because unidimensional.

Several algorithms of TPU have been developed. They differ by the number and the sensitivity of the phases needed to unwrap a given wrapped phase. It has been shown[2] that the "forward exponential method" algorithm with a geometrical progression of the phase sensitivities (between $-2^i\pi$ and $2^i\pi$ with $i = 0, 1, 2, 3, .., n$) is a good compromise between the number of needed phases and the unwrapping reliability. Therefore it has been chosen for our application. The practical implementation of this algorithm is represented in figure 3 for $n = 2$.

3. LABORATORY SETUP

An experimental setup has been developed in our laboratory. It allows the practical implementation of height measurement techniques with structured light. A monochrome CCD camera with 576×768 pixels is placed above the reference plane on which the object is to be measured. The structuration of the light is made by a LCD beamer (SONY SVGA VPL-CS4). Its original optics have been removed and replaced by a telecentric optic. A computer controls both camera data and light structuration. It allows an automatic adaptation of the structuration depending of the object to be measured through a feedback loop (fig.4 a).

4. LINEARIZATION OF THE PROJECTION SYSTEM TRANSFER FUNCTION

Intrinsic conditions of the setup (lighting, structuring element or camera) and extrinsic conditions (nature of the surface to measure) make the global transfer function between the desired intensity we want to project and the perceived intensity by the computer a nonlinear transfer function. This nonlinearity deforms or cuts the

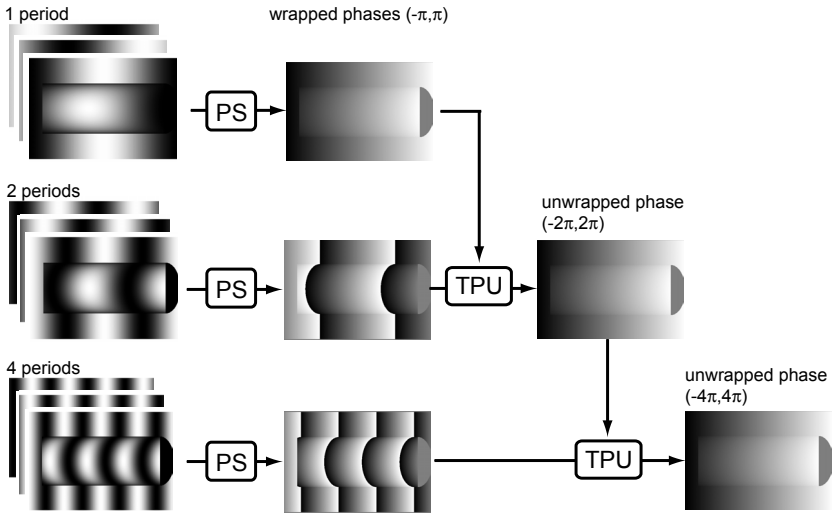

Figure 3. Representation of the temporal phase unwrapping with geometrical progression of the number of periods. The left side represents the intensities from which the phase are computed. The first phase between $-\pi$ and π allows to unwrap the second phase between -2π and 2π. This unwrapped phase allows to unwrap the third phase between -4π and 4π.

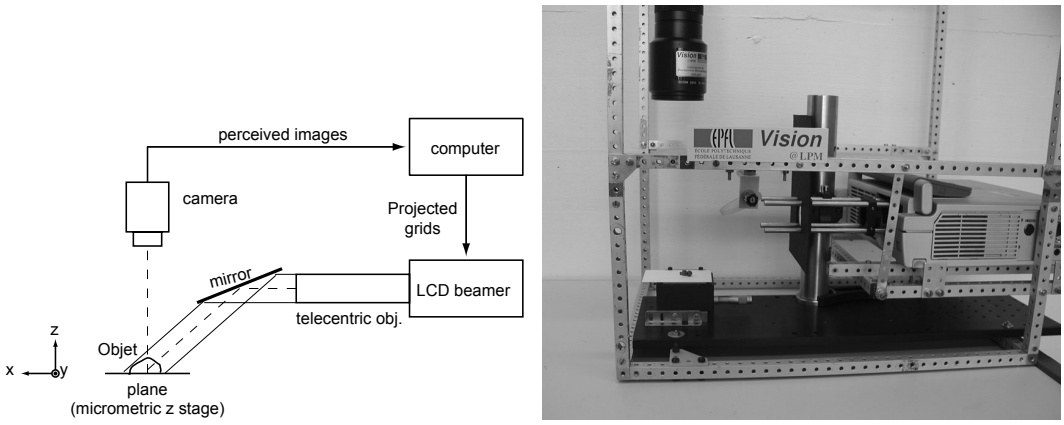

(a) (b)

Figure 4. a) Setup representation with the different elements. b) Practical realisation with global width approximately $45cm$

preceived sinusodal signals. The computed phase is thus no more linear and present some sinusodal deformation (fig.5). These deformations produce local variations of the sensitivity $dz/d\varphi$ and then degrade the accuracy of height measurement. If too high, they can even produce unwrapping errors.

This nonlinearity can be measured and corrected by using a look up table (LUT). This LUT is the inverse function of the system global transfer function. The light structuration we want to project is first computer deformed by the LUT and then reformed by the system. The transfer function composed by LUT and global transfer function can be considered as a linear transfer function (fig.5). Figure 6 shows practical values of the transfer function, LUT and linearized transfer function on a white and black surface. Linearization is possible inside minimum and maximum perceivable values. The transfer function for a given surface can be easily obtained by projecting successively uniform images with growing intensity and recording the perceived intensities. This

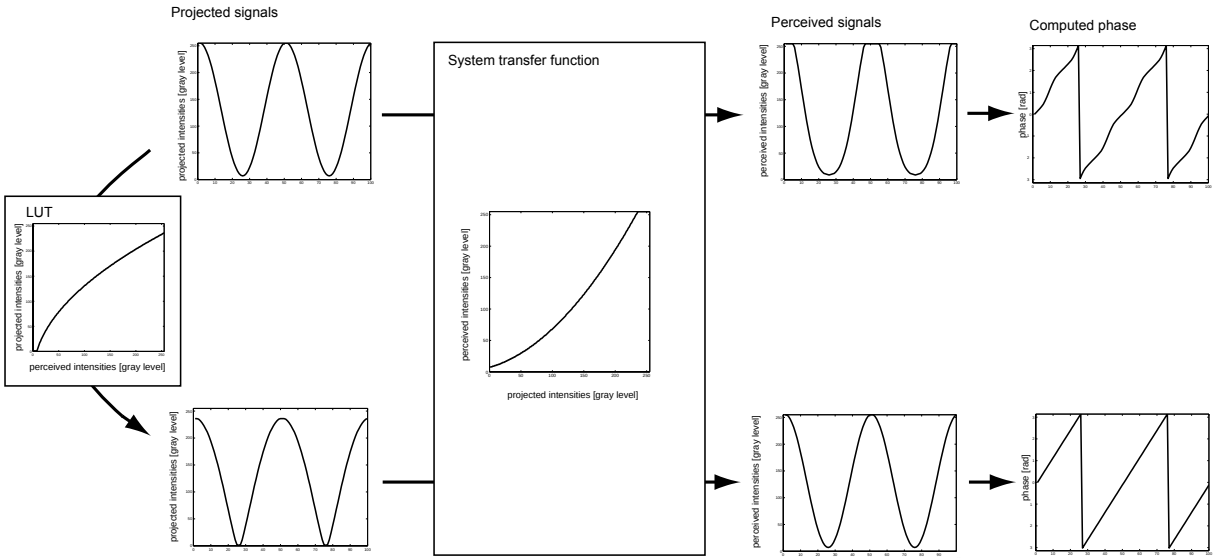

Figure 5. The top of this figure shows the case where a sinusodal signal is directly projected in the system and deformed by the system transfer function. The resulting phase is no more linear. On the bottom, the desired signal is first deformed by the LUT and then projected in the system. The global transfer function becomes linear and the phase produced by the perceived signal is correct.

linearization must be computed again for each new type of surface.

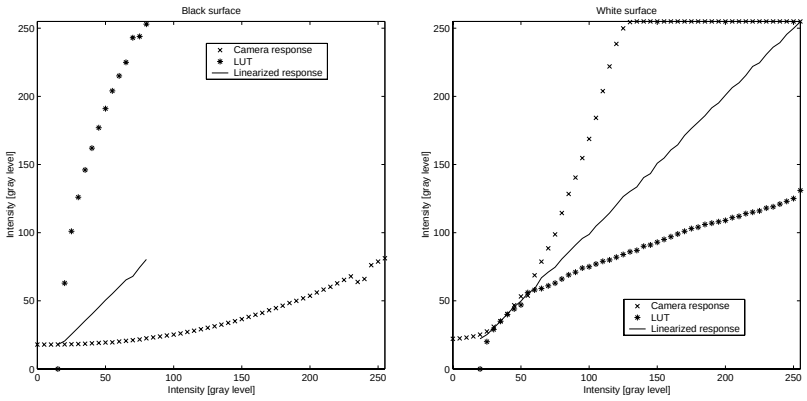

(a) (b)

Figure 6. Linearization of the transfer function between projected and perceived intensities for black and white surfaces by using a look up table. The linearization is only possible between the minimum and maximum perceivable values (30 to 80 for the black surface and 20 to 255 for the white surface).

The use of a LUT does not mean directly that all projected signals will be perceived between the minimum and maximum value of the system response. Indeed, maximum and minimum values of the sinus perceived by the camera will depend of the frequency of the sinus (modulation transfer function). The higher the frequency, the smaller the difference between the maximum and minimum of the perceived sinus. This phenomenon can be seen on figure 7, which presents three perceived sinus with different frequency but all projected between the same values.

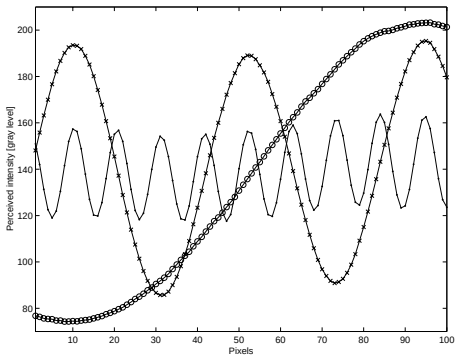

Figure 7. Three perceived sinus with different frequency but all projected between 70 and 200. We see that the higher the frequency, the smaller the difference between the maximum and minimum of the sinus.

5. ESTIMATION OF THE PHASE ERROR

5.1. Origins of phase noises

Even improved by the feedback loop of the LUT, the phase value on a pixel presents always some error. This phase error $\Delta\varphi$ produces a height error Δz following the equation 2. The phase error is composed by a systematic error and a random error. The phase systematic error can be considered to be zero by calibrating the system or making the following hypothesis.

- The incident rays are perfectly collimated.
- The different components of the scanner (optics, LCD, camera) are perfectly aligned.
- The system transfer function is perfectly linearized by a LUT on the usable projected values.
- The depth of field of the projector and camera objectives are much higher than the size of the object.
- The surface of the object to scan is perfectly diffusive and smooth.
- The light source of the projector is considered as spatially uniform on all its surface.

The phase random error comes from intensity random errors and will determine the measurement repeatability. The sources of intensity noises are internal camera noises (shot noise, 1/f noise, fix-pattern noise), digitalization noises (in the framegrabber and in the projector) and time fluctuation of the light source between two images. To be able to predict the repeatability of such 3D measurement system is the best way to increase its performances. For this reason it is important to search propagation mode of intensity random errors on on the phase and find an estimator of the random phase error.

5.2. Estimator of the random phase noise

The following estimation of the random phase noise has been developed for the presented phase stepping equation and phase unwrapping algorithm. Camera and projector images are considered as integer values and phase images as float values.

Random intensity errors can be considered the same on I_1, I_2 and I_3. The intensity on a pixel of the camera is modelled as an ideal intensity with a gaussian noise ΔI with zero mean and constant variance $\sigma^2(\Delta I)$. It can be shown[3] that equation 1 is invariant regarding a constant offset on the 3 intensity values that means $\varphi = f(I_1, I_2, I_3) = f(I_1 + A, I_2 + A, I_3 + A)$ where A is a constant value. The interesting value is only the difference I_{pp} between the maximum and minimum intensities of the sinusodal signal.

The high sensitivity phase between $-n\pi$ and $n\pi$ contains the height information of the object. The reference phase to be subtracted (fig.1 b) is voluntarly neglected because it can be computed as good as we want during

a calibration stage or even be parametrized. For that reason, it is considered to be noiseless. The other phases of lower sensitivity are used only to unwrap the high sensitivity phase. It has been shown in[2] that if a gaussian noise with $\sigma(\Delta\varphi) < 0,2rad$ is present on the phases the unwrapping reliability of the temporal phase unwrapping algorithm we have chosen can be considered as perfect (unwrapping success rate of 100%) for an unwrapped phase between -32π and 32π. This hypothesis is considered to be correct as it will be shown later. The unwrapping being considered as perfect, intensity noise will considered to have the same influence on a phase, whatever is its sensibility. For this reason, the study can be limited to a phase between $-\pi$ and π.

We can see by simulation that a gaussian noise of constant variance $\sigma^2(\Delta I)$ on the 3 intensities I_1, I_2 and I_3 produces a phase noise of variance $\sigma^2(\Delta\varphi)$ for the different phase values, except near the phase limits where an error will rapidly result in a phase jump. So the value of φ can be considered to have no influence on the variance $\sigma^2(\Delta\varphi)$. As we search a practical model, we put some limits depending of the reality. We consider the domain limited by $50 \leq I_{pp} \leq 250$ and $0,1 \leq \sigma^2(\Delta I) \leq 3$. By simulation, we made 630 experiments uniformly spaced on this entire domain. By regression, we found that the estimator

$$\hat{\sigma}(\Delta\varphi) = \sqrt{3} \cdot \frac{\sigma(\Delta I)}{I_{pp}} \tag{3}$$

fit perfectly the simulation with a correlation factor of 0,98 and a mean square error of $\pm 0,02rad$. The highest value of $\hat{\sigma}(\Delta\varphi)$ on the domain is found to be $0,1rad$ (for $\sigma(\Delta I) = 3$ and $I_pp = 50$) which is coherent with the precedent hypothesis concerning the reliability of the unwrapping algorithm.

5.3. Practical validation of the random phase noise estimator

The practical validation of the random phase noise estimator has been made by 50 experiments. Each experiment consisted in scanning 20 times a white ceramic plane and measuring $\sigma(\Delta\varphi)$, $\sigma(\Delta I)$ and I_{pp}. The area of interest on the images includes 140×140 pixels. The intensity noise $\sigma(\Delta I)$ has been increased by adding of software generated noise on projected images or decreased by averaging on several camera images of the same sinusodal projection. The I_{pp} value has been changed by software too. For each experiment, the estimator $\hat{\sigma}(\Delta\varphi)$ were calculated with the $\sigma(\Delta I)$ and I_{pp} measured values and compared with the measured $\sigma(\Delta\varphi)$. We find thus that our model can fit the measured phase noise with a correlation factor of $0,98$ and a mean square error of $\pm 0,007rad$. Figure 8 shows the quality of our estimator.

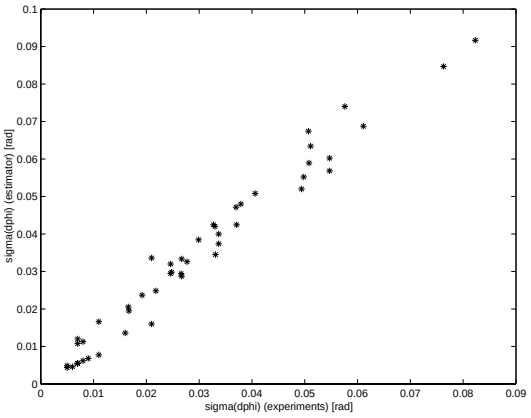

Figure 8. Representation of the quality of our estimator $\hat{\sigma}(\Delta\varphi)$ in the case of 50 experiments inside of the domain limited by $50 < I_{pp} < 250$ and $0,1 < \sigma(\Delta i) < 3$.

5.4. Example

The phase noise estimator is used here in an example. The height difference $\Delta Z = Z_2 - Z_1$ must be measured on the white ceramic part of figure 9 a). A reference value given by a micrometric caliper is $\Delta Z_{ref} = 315\mu m$. A

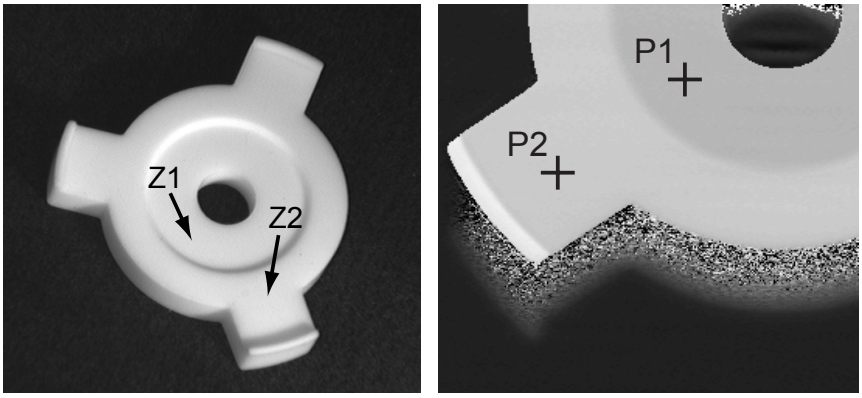

(a) (b)

Figure 9. a) White ceramic part on which we want to measure the height difference $\Delta = Z_2 - Z_1$. b) The height information measured with the setup. The height Z_2 is measured on the pixel P2 and the Z_1 on the pixel P1.

calibration process gives the sensitivity of the setup $dz/d\varphi = 385,5\frac{\mu m}{rad}$. Two pixels P_1 and P_2 are chosen, one on Z_1 and the other on Z_2 (fig.9 b). A first measurement with the setup gives $\Delta Z = 281,78\mu m$. The estimator of the equation 3 gives the confidence interval of this value. Regarding on figure 10, the value $I_{pp} = 200 - 110 = 90$ is estimated. $\sigma(\Delta i)$ is given by the setup. A calibration process gives $\sigma(\Delta i) \simeq 1,5$. The estimator of the random phase error is then $\hat{\sigma}(\Delta\varphi) = 0,03rad$. Combined with the sensitivity, this estimator gives for the pixels P_1 and P_1: $\hat{\sigma}(Z_1) = \hat{\sigma}(Z_2) = \hat{\sigma}(\Delta\varphi) \cdot dz/d\varphi = 11,5\mu m$. The measured value ΔZ is estimated to be correct in a confidence interval of $\pm 3\hat{\sigma}(\Delta Z)$ with $\hat{\sigma}(\Delta Z) = \sqrt{2} \cdot \hat{\sigma}(Z_1) = 16\mu m$. This estimator gives that the mean value on some measurments will be comprised in $\Delta Z = 281,78\mu m \pm 48\mu m$. As a verification, 20 measurements of ΔZ are successively made on the same pixels and give the results presented in figure 11. The systematic error between the measured mean value and the reference value ($315\mu m - 272\mu m = 43\mu m$) can be explained by an imperfect calibration of the setup. The interval of confidence computed by the 20 values is fully coherent with our estimator.

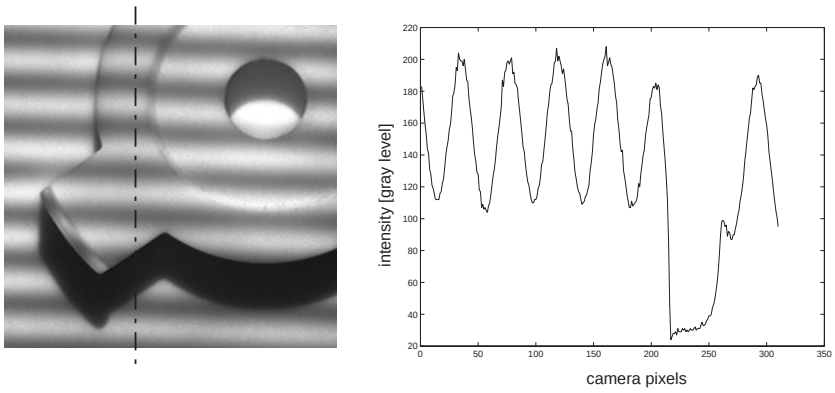

Figure 10. The intensity profil along the dotted line of the left image is computed to determine the I_{pp} value. An approximation is $I_{pp} = 200 - 110 = 90$.

6. CONCLUSIONS

Our experimental 3D measurement system has been presented here, each operation being detailed. In particular, the operations to obtain an unwrapped phase image proportional to the height information of the object are

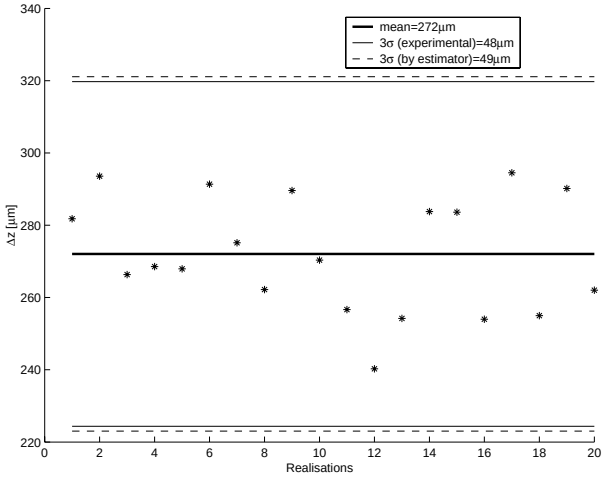

Figure 11. 20 successive measurements of ΔZ shows the reliability of the estimator of random measurement error. The reference value of ΔZ is $315\mu m$. The systematic error of $43\mu m$ can be considered as a consequence of a not perfect calibration of the system.

explained. We show then how the phase quality can be improved by linearizing the projection system transfer function during a calibration process.

A simple estimator of the random phase error $\hat{\sigma}(\Delta\varphi)$ has been also introduced. It gives the confidence interval for the computed height measurement on one pixel. This estimator depends on two parameters to which it is necessary to pay attention in order to predict and thus to improve measurement repeatability. They are the intensity noise $\sigma(\Delta i)$ depending on the system (camera, framegrabber, beamer) and the perceived intensities range I_{pp} for the high frequency grids depending on the color of the object to be measured. We have shown the ability of this estimator, in some practical limits of $(0 \leq \sigma(\Delta i) \leq 3$ and $50 \leq I_{pp} \leq 255)$, to fit the measured values in 50 experiences with a correlation factor of 0,98 and an mean square error of $\pm 0,007 rad$. Finally, we present a practical example of use of our estimator.

REFERENCES

1. H. O. Saldner and J. M. Huntley, "Temporal phase unwrapping: application to surface profiling of discontinuous objects," *Appl. Opt.* **36**(13), pp. 2770–2775, 1997.
2. J. M. Huntley and H. O. Saldner, "Shape measurement by temporal phase unwrapping: comparaison of unwrapping algorithms," *Meas. Sci. Technol.* (8), pp. 986–922, 1997.
3. L.-S. Bieri, "Scanner 3d pour pices microtechniques," student project, EPFL, STI-IPR-LPM, 2001.